

Effects of cosmic strings with delayed scaling on CMB anisotropy

Kohei Kamada,^{1,*} Yuhei Miyamoto,^{2,3,†} Daisuke Yamauchi,^{3,‡} and Jun'ichi Yokoyama^{3,4,§}

¹ *Institut de Théorie des Phénomènes Physiques,
École Polytechnique Fédérale de Lausanne, 1015 Lausanne, Switzerland*

² *Department of Physics, Graduate School of Science,
The University of Tokyo, Tokyo 113-0033, Japan*

³ *Research Center for the Early Universe (RESCEU),
Graduate School of Science, The University of Tokyo, Tokyo 113-0033, Japan*

⁴ *Kavli Institute for the Physics and Mathematics of the Universe (Kavli IPMU),
WPI, TODIAS, The University of Tokyo, Kashiwa, Chiba, 277-8568, Japan*

The network of cosmic strings generated in a phase transition during inflation enters the scaling regime later than that of usual strings. If it occurs after the recombination, temperature anisotropies of the cosmic microwave background (CMB) at high multipole moments are significantly reduced. In this paper, we study such effects qualitatively and show that the constraint on the cosmic string tension from the CMB temperature anisotropies and B-mode polarizations can be relaxed. It is shown to be difficult to explain the recent BICEP2 and POLARBEAR results in terms of signals induced by cosmic strings alone even if we take into account the delayed scaling. However, the inflationary tensor-to-scalar ratio required to explain the observed B-mode signals can be slightly reduced to be consistent with the Planck constraint.

PACS numbers: 98.80.Cq

I. INTRODUCTION

Phase transitions are ubiquitous in the broad fields of physics and, in particular, the key ingredients of high energy physics such as grand unified theories. They predict formation of topological defects [1] through the Kibble mechanism [2] such as monopoles, domain walls, and cosmic strings [3], depending on the symmetry-breaking pattern. Among various types of topological defects, cosmic strings are intriguing objects both in cosmology and high energy physics. They may be produced abundantly in the early Universe but do not dominate the subsequent Universe due to their scaling feature [4], and hence they can leave a variety of traces such as the gravitational-wave background [5] or the cosmic microwave background (CMB) temperature/polarization anisotropies [6, 7] without overclosing the Universe, which gives us rich information about the high energy physics.

In the standard scenario, cosmic strings are formed just after inflation or through thermal phase transition and enter the scaling regime well before the recombination. Therefore, their effects on the CMB temperature/polarization anisotropies are almost independent of the initial condition, which allows us to give general constraints on their properties, such as their tension. However, as discussed in the 1980s [8] and recently pointed out again in a modern context [9], cosmic strings can be formed *during* inflation and they can enter the scaling regime at a later epoch since they are diluted partially during subsequent inflation. In this paper, we show the qualitative effects of this “delayed scaling” of cosmic strings on the CMB anisotropies.

Observations of the CMB temperature anisotropies by WMAP [10] and Planck [11] strongly support the simplest models of inflation, namely, the slow-roll canonical single-field inflation models, and it is found that the cosmic strings alone can explain neither the CMB temperature anisotropies nor the present large scale structure of the Universe. In turn, the CMB temperature anisotropies give a severe constraint on the cosmic string tension of $G\mu \lesssim 1.3 \times 10^{-7}$ for the Nambu-Goto cosmic string model and $G\mu \lesssim 3.2 \times 10^{-7}$ for the Abelian Higgs cosmic string model [12].

Recent observations of the B-mode signal of the CMB polarization anisotropies reported by BICEP2 [13] also give notable suggestions of the physics of the early Universe and the high energy physics. Again, the observed B-mode

*Email: kohei.kamada@epfl.ch

†Email: miyamoto@resceu.s.u-tokyo.ac.jp

‡Email: yamauchi@resceu.s.u-tokyo.ac.jp

§Email: yokoyama@resceu.s.u-tokyo.ac.jp

signal at low multipoles can be explained by the inflationary gravitational waves with the tensor-to-scalar ratio, which directly relates to the energy scale of inflation, being around $r \simeq 0.2$.¹ It is also found that cosmic strings alone cannot fully explain the B-mode signal, since even if we try to fit the BICEP2 B-mode data at the low multipoles by cosmic strings, the dip around $\ell \sim 150$ in the BICEP 2 data is difficult to fit fully and it is incompatible with those at high multipoles observed by POLARBEAR [15] and temperature anisotropies observed by Planck [16].

However, the above conclusion is based on the assumption that the cosmic string network enters the scaling regime well before the recombination. Therefore, it is worth studying how the discussion changes if we take into account the delayed scaling scenario of cosmic strings [8, 9]. In this paper, we study its qualitative effect and show that it relaxes the constraint since the source term for the CMB temperature anisotropies is reduced. Moreover, we find that the B-mode signals may give a stronger constraint on the cosmic string tension, depending on the time when the system enters the scaling regime. Even if we take into account the delayed scaling, it is shown to be difficult to explain the BICEP2 and POLARBEAR B-mode signals by the cosmic string alone, but we also exhibit that they can be fit well by the combination of the cosmic strings, primordial gravitational waves and the gravitational lensing without conflicting with other constraints from the Planck observation.

This paper is organized as follows. In Sec. II, we introduce the delayed scaling scenario using the velocity-dependent one-scale model [4, 17, 18]. In Sec. III, we discuss how it changes the observational signatures in the CMB qualitatively. We also discuss its impact on BICEP2 result. Section IV is devoted to conclusion and discussion. Throughout the paper, our fiducial model is the standard Λ CDM cosmological model with the cosmological parameters $\Omega_b h^2 = 0.022161$, $\Omega_m h^2 = 0.11889$, and $h = 0.6777$ with $\Delta_{\mathcal{R}}^2 = 2.216 \times 10^{-9}$ and $n_s = 0.96$, at $k_0 = 0.05 \text{Mpc}^{-1}$, which is the best-fit model of the Planck 2013 data combined with the polarization of WMAP, other high- ℓ observations, and the baryon acoustic oscillation [19].

II. DELAYED SCALING SCENARIO

Let us first summarize the delayed scaling scenario. Symmetries are naturally restored during inflation due to the ‘‘Hubble-induced’’ mass for the Higgs field responsible for the symmetry breaking² coming from, for example, the direct coupling to the inflaton, the nonminimal coupling to Ricci scalar [8], or the Planck suppressed interaction in the F-term inflation [9]. If the induced mass is larger than the amplitude of its tachyonic zero-temperature mass, the Higgs field settles down to the origin during inflation and the symmetry is restored. In the case the induced mass decreases with time significantly enough, during inflation it can become smaller than the amplitude of the zero-temperature mass and cosmic strings can be formed thorough the phase transition. In this case, they are diluted and their correlation length and mean separation expand exponentially until the end of inflation. As a result, their average distances become much larger than the Hubble length at the end of inflation. This large separation allows the cosmic string network to enter the scaling regime, where the characteristic scale of the string network remains constant relative to the Hubble length, at a later time. This is because the scaling regime is achieved after the characteristic length of the string network becomes smaller than the Hubble length and the energy of infinite strings starts to be converted into small string loops.

In principle, numerical simulations are necessary to study how the system enters the scaling regime in this delayed scaling scenario. Since it will need a huge computation, here we instead evaluate the evolution of the cosmic string network using the one-scale model [4, 17, 18] as a first step. In the (velocity-dependent) one-scale model [17, 18], the correlation length of the infinite string L , which represents both the typical curvature radius of infinite strings and their mean separation, obeys the evolution equation

$$\frac{dL}{dt} = (1 + v^2)HL + \frac{1}{2}\tilde{c}v. \quad (1)$$

Here t is the physical time, $H = \dot{a}/a = H_0(\Omega_m a^{-3} + \Omega_r a^{-4} + \Omega_\Lambda)^{1/2}$ is the Hubble parameter, v is the root mean square of the velocity of infinite string, and $\tilde{c} = 0.23$ is the numerical parameter that represents the loop formation efficiency [18]. We set the scale factor $a = 1$ today. H_0 is the present Hubble parameter, and Ω_m, Ω_r , and Ω_Λ are the present density parameters of the nonrelativistic matter, relativistic matter, and the cosmological constant, respectively. The

¹ Many authors use the Planck constraint on the tensor-to-scalar ratio $r < 0.11$ at $k_0 = 0.002 \text{Mpc}^{-1}$ for $n_t = -r/8$ [11] to compare it with the BICEP2 result. In Refs. [14], however, it has been shown that at our pivot scale $k_0 = 0.05 \text{Mpc}^{-1}$ for $n_t = 0$, the Planck data give the constraint as $r < 0.135$. Therefore we take $r = 0.135$, $n_t = 0$ throughout this paper when we show effects of inflationary tensorial perturbations.

² For the similar studies on the monopole production during inflation, see Ref. [20].

velocity v evolves with the evolution equation,

$$\frac{dv}{dt} = (1 - v^2) \left(\frac{\tilde{k}}{L} - 2Hv \right), \quad (2)$$

with $\tilde{k} = (2\sqrt{2}/\pi)((1 - 8v^6)/(1 + 8v^6))$ being the momentum parameter that represents the acceleration effect due to the curvature of the strings [18].

Although the velocity-dependent one-scale model, characterized by Eqs. (1) and (2), is intended to describe evolution of the string network formed by the conventional Kibble mechanism, these equations also reproduce the initial evolution of string segments before entering the scaling regime correctly; that is, v tends to 0 when $L \gg H^{-1}$ and L evolves in proportion to the scale factor, if we take an appropriate “initial” time with a large initial correlation length $L_{\text{ini}} \gg H_{\text{ini}}^{-1}$. Note that the CMB anisotropies induced by cosmic strings are insensitive to their behaviors in the earlier epoch, and we do not have to follow their evolution from the end of inflation. It is not clear if the one-scale model, where we assume that the typical curvature of the infinite strings and their mean separation are equal, holds just after inflation, but we expect it gives a good approximation since the Hubble parameter during inflation is the unique parameter to determine the string configuration when they are formed. The validity of this model, especially in the intermediate regime, should nevertheless be investigated through numerical simulations with appropriate initial conditions, which is beyond the scope of the present paper, and we use (1) and (2) throughout.

Figure 1 shows the typical evolution of the correlation length relative to the Hubble length H^{-1} with a different (relatively large) initial correlation length. Hereafter we set $z = 2.3 \times 10^7$ as initial time. The initial velocity is set to $v = 0$ except for the bottom line, which represents the standard, always-scaling case with initial velocity $v = 0.65$. While we chose such initial velocities, we also confirmed that the evolution of the correlation length is almost independent of the initial velocity, since the velocity decreases vanishingly and it loses its initial information quickly. As mentioned above, when L is larger than the horizon scale, it simply evolves in proportion to a . In terms of the redshift z , L/H^{-1} is proportional to z in the radiation dominated era ($z \gg z_{\text{eq}}$) and $z^{1/2}$ in the matter dominated era ($z \ll z_{\text{eq}}$), where $z_{\text{eq}} \approx 3400$ is the redshift at the matter-radiation equality. We can also see that it takes a few orders of redshift for the system to enter the scaling solution completely, which will be important for the observational signatures. Since this result shows the general feature of the evolution of the correlation length on superhorizon scales,

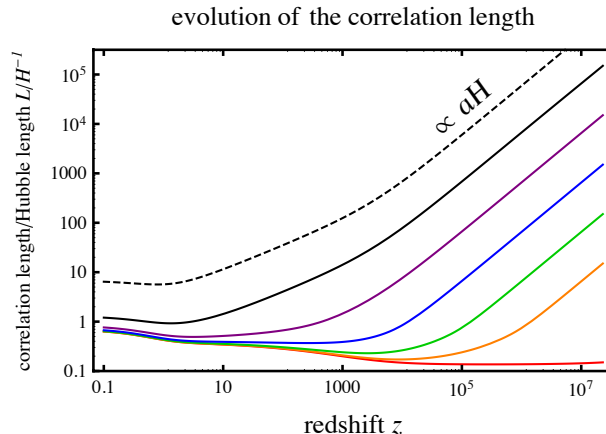


FIG. 1: The evolution of the correlation length relative to the Hubble length. Compared to the dashed black line which is proportional to aH , we can easily see that the correlation length evolves proportional to the scale factor on superhorizon scales.

it strongly suggests that even if the correlation length is much larger than the Hubble length just after inflation, the system gradually approaches the scaling solution and at a relatively late epoch, say $z = 10^3$ or later, starts to evolve in accordance with the scaling rule depending on the epoch of the phase transition during inflation. Note that if the phase transition takes place when the present horizon scale exited the horizon during inflation, the correlation length would become the horizon scale again today, since its initial correlation length can be estimated by the horizon scale at that time. Therefore, cosmic strings formed several e -folds after the current Hubble scale went out of the horizon during inflation would enter the scaling regime after the recombination.³ To evaluate the onset time of scaling, we

³ In principle, the initial correlation length can be calculated from the model parameters, (see, *e.g.*, Ref. [9]), but the inflation model must

calculate the redshift when the correlation length L becomes $2L_{\text{scaling}}$, as well as the redshift when the correlation length falls shorter than the horizon. Here L_{scaling} is the correlation length of the scaling network, which corresponds to the bottom line in Fig. 1. In Fig. 2, we show these redshifts as a function of the initial correlation length. This figure shows that there arises an intermediate epoch before the complete entrance into the scaling regime, which may be important for the CMB anisotropies.

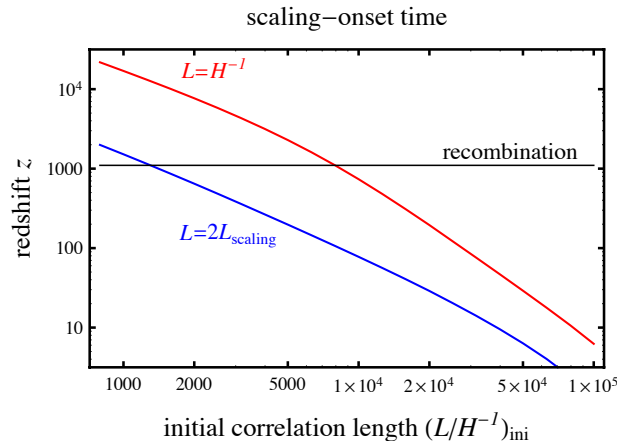


FIG. 2: The redshift at which the system enters the horizon and approaches the scaling solution as a function of the initial correlation length.

III. CMB FROM COSMIC STRINGS WITH DELAYED SCALING

We now study the signatures of cosmic strings on the CMB anisotropies in the delayed scaling scenario. Here we use a code based on the public code CMBACT [21]. For comparison, we calculate the inflationary contributions using CAMB [22].

A. Temperature anisotropies

Let us discuss first the effect of strings with delayed scaling on the temperature anisotropies to investigate how the constraint on the string tension changes qualitatively. Varying the initial correlation length, we show the angular power spectrum for the CMB temperature anisotropies induced by cosmic strings in the left panel in Fig. 3. For illustrative purposes, from top to bottom, we adopt the string tension $G\mu = 3 \times 10^{-7}$ with the initial correlation lengths as $(L/H^{-1})_{\text{ini}} = 1.5, 7.5 \times 10^3, 4.5 \times 10^4$, and 1.5×10^5 . With the help of Fig. 2, we can estimate the scaling-onset time for each initial correlation length. Hence, we can treat the last three cases as the delayed scaling cases, while the first one corresponds to the system which already realizes the scaling by the time of the recombination.

One can see that the contributions from the strings give a single broad peak. It moves to the lower multipoles and the power-law behavior on small scales decays as the initial correlation length becomes large. Thus, increasing $(L/H^{-1})_{\text{ini}}$ decreases the string-induced small-scale signals significantly. On large-scale signals, $\ell \sim 10$, we also see a slight decrease of the amplitude of the temperature anisotropies.

Now we interpret the above features of the strings with delayed scaling. In considering the effect of the long string network on the CMB, we can treat it as if it consisted of many “string segments” with length L [21]. Since in the one-scale model the number density of such segments of cosmic strings is estimated as L^{-3} , the number density and the resultant contributions to the CMB fluctuations are small when the correlation length is large. With this fact in our mind, we can presume the reason of the significant decrease at high multipoles as follows. In the standard scenario, the peak around $\ell \sim 500$ is generated by strings at the recombination [23]. Therefore, when the correlation length of strings is very large at the recombination, the number density of strings and their contributions to such

be specified, which is beyond the scope of this study.

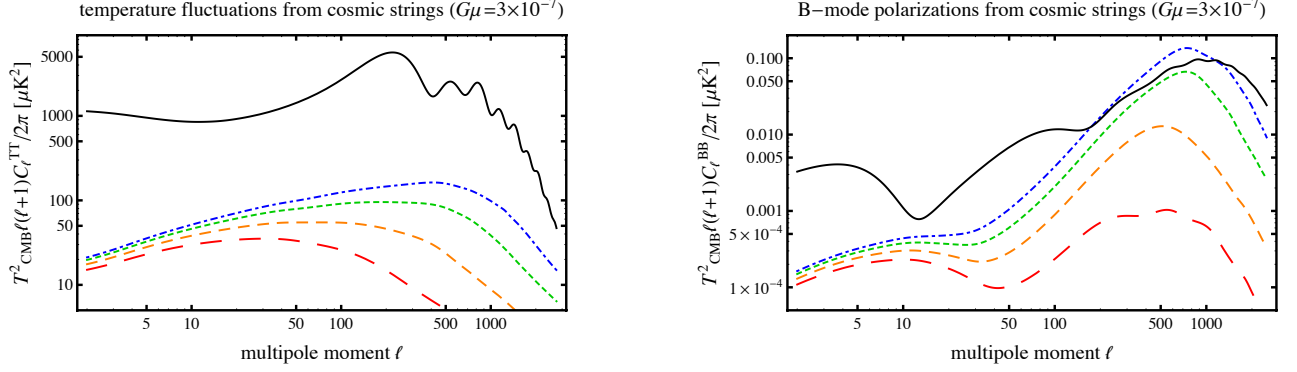


FIG. 3: Angular power spectra for the temperature/B-mode polarization fluctuations induced by cosmic strings with $G\mu = 3 \times 10^{-7}$. From top (blue dot-dashed) to bottom (red long dashed), we take the initial correlation length $(L/H^{-1})_{\text{ini}} = 1.5, 7.5 \times 10^3, 4.5 \times 10^4$, and 1.5×10^5 . In the left panel, the contributions from inflationary perturbations are shown in the black solid line, for comparison. In the right panel, the black solid line corresponds to the primordial gravitational waves with $r = 0.135$ and gravitational lensing. Note that the overall amplitudes scale as $(G\mu)^2$.

high multipoles become significantly small. In this case, since the number density of strings is negligibly small until the system enters the scaling regime, the position of the peak would be determined by the onset time of scaling and get lower. Next, we consider why we see only a slight decline at low multipoles. The signal in these scales would be mainly induced by the cosmic strings at late times. As we can see from Figs. 1 and 2, it takes time for the system to enter the complete scaling regime and a larger initial correlation length turns into a slightly larger correlation length and hence slightly smaller number density at later times. As a result, there is only a slight decrease of the amplitude of the string-induced large-scale signals.⁴

Here we comment more on the number of cosmic string segments. We define the total number of cosmic strings between the last scattering surface and us as

$$\begin{aligned} & \int_0^{r_{\text{dec}}} 4\pi a^3 r^2(z) dr \frac{1}{L^3(z)} \\ &= \int_0^{1100} \frac{dz}{H(z)} \frac{4\pi}{(1+z)^3} \left(\int_0^z \frac{1}{H(z')} dz' \right)^2 \frac{1}{L^3(z)}, \end{aligned} \quad (3)$$

where $r(z)$ is a comoving distance to the surface whose redshift is z ,

$$r(z) = \int_0^z \frac{1}{H(z')} dz'. \quad (4)$$

In Fig. 4, we show the dependences on the initial correlation length for the total number and its partial components which are expected to give dominant contributions to large- and small-scale fluctuations. We can explicitly see that the total number of cosmic strings is significantly reduced if we set the initial correlation length very large. We can also see that for $(L/H^{-1})_{\text{ini}} = 10^3 \sim 10^5$, the number of string segments around the recombination drastically decreases, whereas those around reionization show a milder decrease. This is consistent with the behavior of the power spectrum of the CMB temperature and polarization fluctuations in Fig. 3. Note that for the large initial correlation length, the cosmic variance becomes so large that we have to be careful in comparing theoretical, ensemble-averaged quantities and observations.

With the discussion given above, we then conclude that the constraint on the string tension is relaxed in the delayed scaling scenario. We show some quantitative constraints in Fig. 5. Solid lines in the left panel of Fig. 5 show the upper bound on the string tension from the CMB temperature anisotropies, which was obtained from the condition

⁴ Note that while the number of strings is reduced, each segment contributes to larger multipoles, since we expect the scale of dominant fluctuations generated by each segment to be proportional to L^{-1} . Therefore the delayed scaling effect is not fully determined by the number density.

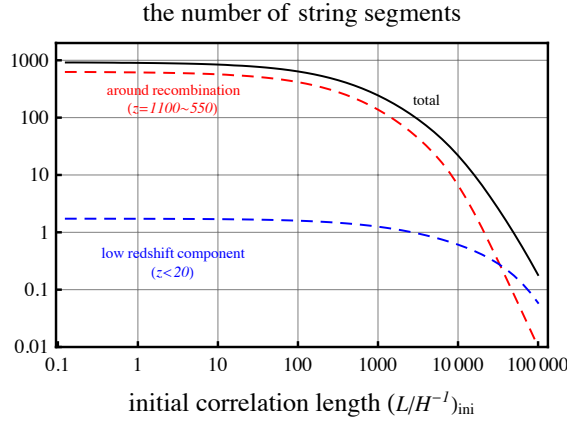


FIG. 4: The solid black line represents the total number of string segments from the recombination to the present. The dashed red line, which corresponds to the number of strings near the last scattering surface, rapidly decreases as the initial correlation length becomes large. We also plot the number of strings in the low-redshift region ($0 \leq z \leq 20$) by a dashed blue line. Its dependence on the initial correlation length is smaller than that of strings being around the recombination.

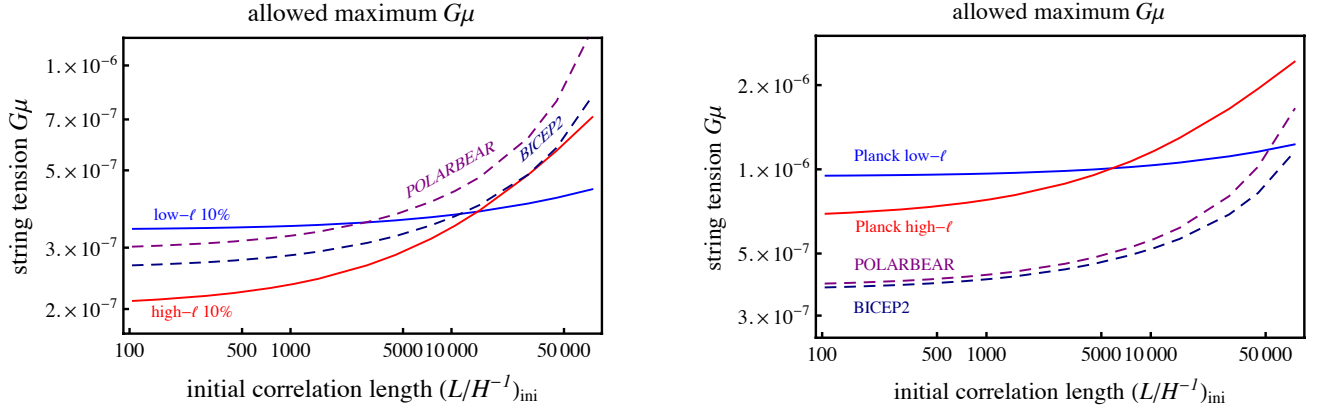


FIG. 5: The contour for the constraint on the string tension $G\mu$ as a function of the initial correlation length $(L/H^{-1})_{\text{ini}}$. In the left panel, constraints obtained from the condition that the string temperature anisotropies do not exceed 10% of the primordial one are shown in red (small scale, $2250 \leq \ell \leq 2450$) and blue (large scale, $\ell \leq 50$). The dashed dark blue (dark red) line shows the excluded region from the condition that the string polarizations added to the lensing effect do not exceed the spectra measured by the BICEP2 (POLARBEAR) data. In the right panel, more conservative limits on $G\mu$ are depicted from the condition that the temperature and polarization fluctuations generated only by cosmic strings (namely, without inflationary temperature fluctuations and gravitational waves, and the lensing effect) do not exceed the observed values.

that the string-induced temperature anisotropies would not exceed 10%⁵ of the values given by the fiducial Λ CDM model. The red line is the constraint from the small-scale signals, whereas the blue line is that from the large-scale counterparts. We can see that the small-scale signals give a stronger constraint for smaller initial correlation length and large-scale signals give a stronger one for larger initial correlation length. In particular, for $(L/H^{-1})_{\text{ini}} = 10^4$, the constraint on $G\mu$ is $G\mu \lesssim 3.4 \times 10^{-7}$. Although the resultant constraint would depend on the criterion of the condition, the generic features are expected to remain the same. For comparison, in the right panel of Fig. 5 we also show more conservative limits coming from the condition that the temperature fluctuation created solely by cosmic strings (without inflationary perturbations) would not exceed the observed value by Planck. We can see that although the quantitative constraints are very different, shapes of the constraint lines do not change significantly. That is, the constraint from the small scales is more severe than that from the large scales for smaller initial correlation length,

⁵ The precision of the data provided by Planck is about 10% including cosmic variance for $\ell \lesssim 50$ and $2250 \lesssim \ell \lesssim 2450$.

and the opposite is the case for longer initial correlation length.

In summary, we emphasize that the high- ℓ temperature power spectra from cosmic strings are suppressed due to the delayed scaling, which loosens the constraint on the string tension. Note that the present constraint on the string tension comes from high- ℓ data.

B. B-mode polarizations

Let us discuss the effect of the delayed scaling on the CMB polarization signals. The right panel of Fig. 3 shows the angular power spectra for the B-mode polarization from strings with delayed scaling with $G\mu = 3 \times 10^{-7}$ and the initial correlation lengths $(L/H^{-1})_{\text{ini}} = 1.5, 7.5 \times 10^3, 4.5 \times 10^4$ and 1.5×10^5 . The resultant spectrum has two broad peaks, whose positions are expected to be determined by the contributions from the scattering of photons during the reionization (the peak at lower multipole) and the recombination epochs (the peak at higher multipole). We can see that the main peak at higher multipole rather than the peak at lower multipole is sensitive to the initial correlation length. Relatively large initial correlation length in general leads to the decrease in the B-mode signals on small scales. This is mainly because increasing $(L/H^{-1})_{\text{ini}}$ leads to the decrease in the number of strings during the recombination. We also see that the scale of the peak does not shift so much according to the change of the initial correlation length. If the position of the peak is determined only by the correlation length L at the recombination, we expect it would be located at much lower multipole. The reason for this not being the case would be the fact that we do not observe the snapshot of the string network itself at the recombination which does not occur instantaneously. In contrast, the peak at lower multipole is not suppressed drastically. This would be understood by the same discussion in the previous subsection. From Fig. 4, we can see that the number of strings at the reionization is less dependent on the initial correlation length than those at the recombination for the initial correlation length we adopted here.

Let us consider the constraint on the string tension $G\mu$ from the B-mode polarizations. To keep the constraint conservative, we assume $r = 0$. In this case, the most stringent constraint from the B-mode polarizations comes from the signals observed by BICEP2 at $\ell \sim 320$ and by POLARBEAR at $\ell \sim 700$. Hence we find that in the delayed scaling scenario the constraint on $G\mu$ from the B-mode polarization can also be relaxed. Requiring that the string-induced B-mode signals with (without) the lensing effect do not exceed the data measured by BICEP2 and POLARBEAR, we plot in the left (right) panel of Fig. 5 each of these upper bounds on the string tension as a function of the initial correlation length.⁶ We find the constraint imposed by the B-mode polarizations is comparable to or more severe than that by the temperature fluctuations, depending on the criterion of the condition. Since the small-scale temperature fluctuations are usually dominated by the contributions from point sources, the Sunyaev-Zel'dovich effect and other secondary effects, the B-mode measurement would be a complementary probe for strings with delayed scaling and also help to check the systematics in the derived constraint from the temperature fluctuations. Moreover, the different features between the string-induced temperature fluctuations and polarizations provide the different dependence on the string parameters. These different behaviors suggest that the combined analysis would be quite essential not only to obtain a tighter constraint on string parameters, but also to break the parameter degeneracies. This is left for a future study.

Before closing this section, we attempt to match the string-induced B-mode spectrum to the BICEP2 and POLARBEAR data. First we comment on the string-only model with gravitational lensing to compare the observational data. As can be seen from the right panel of Fig. 3, cosmic strings cannot create a small peak around $\ell \sim 50$ and a small dip around $\ell \sim 150$, which are seen in the BICEP2 result, though they can contribute to the higher multipoles. Hence, even if we take into account the delayed scaling scenario, it is difficult to explain BICEP2 data only by cosmic strings since it cannot explain the BICEP2 result for both $\ell \lesssim 150$ and $\ell \gtrsim 150$ simultaneously, as well as POLARBEAR results. Then, we consider the case in which both cosmic strings and primordial gravitational waves contribute to the B-mode signals. Figure 6 shows the angular power spectra of the B-mode polarization fluctuations induced by the cosmic strings with $G\mu = 3 \times 10^{-7}$ in the delayed scaling scenario [$(L/H^{-1})_{\text{ini}} = 7500$], as well as that induced by the primordial gravitational waves with $r = 0.135$ and the gravitational lensing. We also plot the B-mode signals observed by BICEP2 and POLARBEAR.

We find this combination of three types of tensor perturbations significantly improves the fit to BICEP2 data. As a demonstration, we show $\delta\chi^2$ as a function of $G\mu$ and $(L/H^{-1})_{\text{ini}}$ in Fig. 7, comparing the prediction of the delayed scaling scenario added to the primordial gravitational waves $r = 0.135$ and the gravitational lensing with that of the primordial gravitational waves $r = 0.2$ and gravitational lensing without strings. It decreases as much as $\delta\chi^2 \approx -9$ with two additional parameters, $G\mu$ and $(L/H^{-1})_{\text{ini}}$ as far as fitting to BICEP2 data is concerned. We note here

⁶ Here we omit the third band of POLARBEAR at $\ell \sim 1500$ that gives a negative value.

that compared to the conventional early scaling case, the delayed scaling model predicts suppression of the power spectra at high ℓ ($\ell \gtrsim 200$). Therefore, we conclude that although the improvement of χ^2 is almost the same as the initially scaling case, which has been studied in Ref. [16], the detailed effects are different. Moreover, we expect that the delayed scaling would be favored compared to the conventional model if temperature data are included. This is because in the delayed scaling scenario, a large enough string tension to fit the B-mode data, which is excluded in the conventional early scaling scenario, is still allowed owing to the suppression of the temperature power spectra at high ℓ as we have seen in the previous subsection.

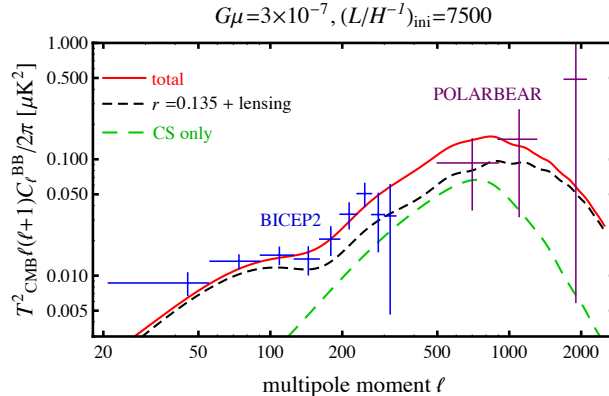


FIG. 6: B-mode polarization angular power spectra for gravitational lensing with primordial gravitational waves ($r = 0.135$, $n_t = 0$, black short-dashed line) and contributions from cosmic strings with delayed scaling [$G\mu = 3 \times 10^{-7}$, $(L/H^{-1})_{\text{ini}} = 7500$, green long-dashed line]. If we combine them, the favorable value of r would be smaller than 0.2.

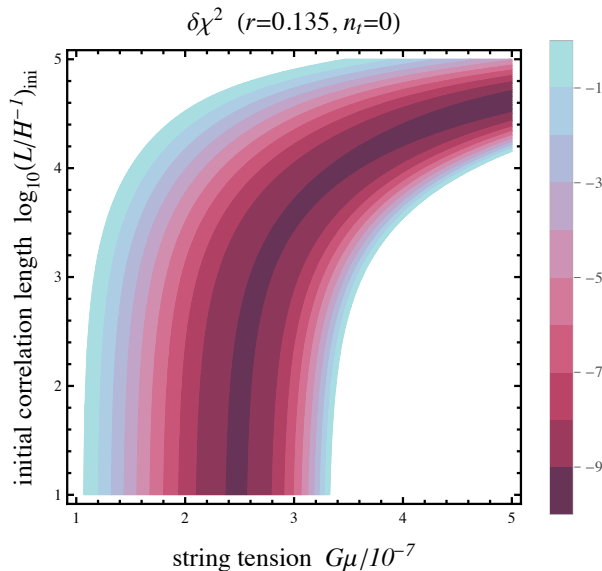


FIG. 7: The contour of the difference of χ^2 between the prediction in taking $r = 0.2$ without strings ($\chi^2 \approx 15$) and that of cosmic strings with delayed scaling added to that for $r = 0.135$ based on BICEP2 data. The value of χ^2 gets worse in blank regions.

IV. CONCLUSION AND DISCUSSION

In this paper we have studied the evolution of “delayed scaling” strings and its potential impacts on CMB measurements such as Planck, BICEP2 and POLARBEAR. We have also discussed how the constraints on the parameters change. The key is to consider the scenario in which cosmic strings are formed not after but *during* inflation. Such

strings have exponentially large separation due to the dilution during the subsequent inflation and their evolution is quite different from that of strings which enter the scaling regime at an earlier epoch.

We have traced typical evolution of the string network by solving the velocity-dependent one-scale model. We have shown that if we take the relatively large correlation length at the initial time, the correlation length decays as a rather than $1/H$ at an earlier epoch and it takes a few orders of redshift for the system to enter the scaling regime (Fig. 1).

Based on the evolution of the network, we have calculated the angular power spectra for the string-induced temperature anisotropies and B-mode polarizations. We found that the large initial correlation length and the consequent delay of the entrance into the scaling regime allow the decrease in the number of strings at an earlier epoch, leading to the decay of the string signals mainly on higher multipoles (Fig. 3). As a result, the delayed scaling scenario can relax the constraint on the string tension from the measurements for both the temperature anisotropies and the B-mode polarizations.

We have further discussed the features of the B-mode signals produced by strings. For the string-only model with the contribution of the gravitational lensing, it is difficult to explain both BICEP2 and POLARBEAR data fully since the shape of the spectrum from cosmic strings still lacks powers on lower multipoles as required by the BICEP2 results. On the other hand, we have shown that delayed string contribution added to the primordial gravitational waves with smaller tensor-to-scalar ratio being consistent with Planck improves the fit to the BICEP2 data, although more data and its analysis are certainly required to draw final conclusion.

Throughout the paper, we have assumed several idealizations. In particular, our results are based on the velocity-dependent one-scale model, though it is not obvious that this model characterizes the evolution of strings with delayed scaling. The uncertainty may lead to significant changes in the observables. Studies on the network model for the strings with delayed scaling should be further improved for future applications to CMB measurements.

Acknowledgments

The authors thank D. Figueroa, M. Hindmarsh, and T. Suyama for helpful discussions and comments. This work has been supported in part by the JSPS Postdoctoral Fellowships for Research Abroad (K.K.), the Grant-in-Aid for JSPS Fellows No. 259800 (D.Y.), JSPS Grant-in-Aid for Scientific Research No.23340058 (J.Y.), and JSPS Research Fellowships for Young Scientists (Y.M.).

-
- [1] A. Vilenkin and E. P. S. Shellard, Cambridge University Press, Cambridge, England, 2000; M. B. Hindmarsh and T. W. B. Kibble, Rept. Prog. Phys. **58**, 477 (1995) [arXiv:hep-ph/9411342].
 - [2] T. W. B. Kibble, J. Phys. A **9** (1976) 1387.
 - [3] Y. B. Zeldovich, Mon. Not. Roy. Astron. Soc. **192**, 663 (1980); A. Vilenkin, Phys. Rev. Lett. **46**, 1169 (1981) [Erratum-ibid. **46**, 1496 (1981)].
 - [4] T. W. B. Kibble, Nucl. Phys. B **252**, 227 (1985) [Erratum-ibid. B **261**, 750 (1985)].
 - [5] A. Vilenkin, Phys. Lett. B **107**, 47 (1981).
 - [6] A. Albrecht, R. A. Battye and J. Robinson, Phys. Rev. Lett. **79**, 4736 (1997) [astro-ph/9707129].
 - [7] U. Seljak, U. -L. Pen and N. Turok, Phys. Rev. Lett. **79**, 1615 (1997) [astro-ph/9704231]; W. Hu and M. J. White, Phys. Rev. D **56**, 596 (1997) [astro-ph/9702170].
 - [8] G. Lazarides, Q. Shafi, Phys. Lett. **B148**, 35 (1984); Q. Shafi, A. Vilenkin, Phys. Rev. **D29** (1984) 1870; E. T. Vishniac, K. A. Olive, D. Seckel, Nucl. Phys. **B289** (1987) 717; L. A. Kofman, A. D. Linde, Nucl. Phys. **B282** (1987) 555; J. Yokoyama, Phys. Lett. **B212** (1988) 273; Phys. Rev. Lett. **63** (1989) 712. See also: M. Nagasawa and J. Yokoyama, Nucl. Phys. B **370** (1992) 472; K. Freese, T. Gherghetta, H. Umeda, Phys. Rev. **D54** (1996) 6083 [arXiv:hep-ph/9512211].
 - [9] K. Kamada, Y. Miyamoto and J. Yokoyama, JCAP **1210**, 023 (2012) [arXiv:1204.3237 [astro-ph.CO]]; A. Linde, Phys. Rev. D **88**, 123503 (2013) [arXiv:1303.4435 [hep-th]].
 - [10] G. Hinshaw *et al.* [WMAP Collaboration], Astrophys. J. Suppl. **208**, 19 (2013) [arXiv:1212.5226 [astro-ph.CO]].
 - [11] P. A. R. Ade *et al.* [Planck Collaboration], arXiv:1303.5082 [astro-ph.CO].
 - [12] P. A. R. Ade *et al.* [Planck Collaboration], arXiv:1303.5085 [astro-ph.CO].
 - [13] P. A. R. Ade *et al.* [BICEP2 Collaboration], Phys. Rev. Lett. **112**, 241101 (2014) [arXiv:1403.3985 [astro-ph.CO]].
 - [14] B. Audren, D. G. Figueroa and T. Tram, arXiv:1405.1390 [astro-ph.CO].
 - [15] P. A. R. Ade *et al.* [The POLARBEAR Collaboration], arXiv:1403.2369 [astro-ph.CO].
 - [16] J. Lizarraga, J. Urrestilla, D. Daverio, M. Hindmarsh, M. Kunz and A. R. Liddle, Phys. Rev. Lett. **112**, 171301 (2014) [arXiv:1403.4924 [astro-ph.CO]]; A. Moss and L. Pogosian, Phys. Rev. Lett. **112**, 171302 (2014) [arXiv:1403.6105 [astro-ph.CO]].
 - [17] C. J. A. P. Martins and E. P. S. Shellard, Phys. Rev. D **54**, 2535 (1996) [hep-ph/9602271].

- [18] C. J. A. P. Martins and E. P. S. Shellard, Phys. Rev. D **65**, 043514 (2002) [hep-ph/0003298].
- [19] P. A. R. Ade *et al.* [Planck Collaboration], arXiv:1303.5076 [astro-ph.CO].
- [20] J. Yokoyama, Phys. Lett. B **231**, 49 (1989); K. Kamada, K. Nakayama and J. Yokoyama, Phys. Rev. D **85**, 043503 (2012) [arXiv:1110.3904 [hep-ph]].
- [21] L. Pogosian and T. Vachaspati, Phys. Rev. D **60**, 083504 (1999) [astro-ph/9903361].
- [22] A. Lewis, A. Challinor and A. Lasenby, Astrophys. J. **538**, 473 (2000) [astro-ph/9911177].
- [23] N. Bevis, M. Hindmarsh, M. Kunz and J. Urrestilla, Phys. Rev. D **82**, 065004 (2010) [arXiv:1005.2663 [astro-ph.CO]].